Eur. Phys. J. B **53**, 529–536 (2006)
DOI: 10.1140/epjb/e2006-00401-9

THE EUROPEAN PHYSICAL JOURNAL B

Role of the driving frequency in a randomly perturbed Hodgkin-Huxley neuron with suprathreshold forcing

E.V. Pankratova[1,a], V.N. Belykh[1], and E. Mosekilde[2]

[1] Mathematical Department, Volga State Academy, Nizhny Novgorod, 603600, Russia
[2] Department of Physics, The Technical University of Denmark, 2800 Kongens Lyngby, Denmark

Received 29 March 2006 / Received in final form 3 October 2006
Published online 6 November 2006 –

Abstract. The present paper examines the influence of the forcing frequency on the response of a randomly perturbed Hodgkin-Huxley system in the realm of suprathreshold amplitudes. Our results show that, in the presence of noise, the choice of driving frequency can seriously affect the precision of the external information transmission. At the same level of noise the precision can either decrease or increase depending on the driving frequency. We demonstrate that the destructive influence of noise on the interspike interval can be effectively reduced. That is, with driving signals in certain frequency ranges, the system can show stable periodic spiking even for relatively large noise intensities. Here, the most accurate transmission of an external signal occurs. Outside these frequency ranges, noise of the same intensity destroys the regularity of the spike trains by suppressing the generation of some spikes. On the other hand, we show that noise can have a reconstructive role for certain driving frequencies. Here, increasing noise intensity enhances the coherence of the neuronal response.

PACS. 87.10.+e General theory and mathematical aspects – 05.40.-a Fluctuation phenomena, random processes, noise, and Brownian motion – 05.45.-a Nonlinear dynamics and chaos

1 Introduction

Nerve cells transform stimuli from the external world into trains of spikes that propagate from cell to cell to be processed in the central nervous system. From neurophysiological experiments we know that signal processing occurs in the presence of multiple sources of noise, such as random opening and closing transitions of the ion channels in the cellular membrane, fluctuations of membrane parameters, external input variability, etc. [1]. Nonetheless, neurons display an amazing ability to react appropriately to external perturbations and to exhibit reliable activity patterns [2,3]. Investigation of the influence of noise on spike generation in the presence of different external forcing signals is therefore of significant interest, and a large number of studies have already been devoted to this problem [2–8,11–28]. In particular, the effect of periodic stimulation of neurons has been extensively studied within the framework of different lines of research: from a classical resonance (mode locking) perspective [7–10], from a stochastic resonance point of view [11–13], and in terms of the spike time precision approach [20–24]. It has been shown that noise can play both a constructive (mediated by the stochastic resonance effect for the case of a weak periodic signal) [11–13] and a destructive role for suprathreshold signals [14–18]. The complex interactions between noise and deterministic dynamics has recently been examined by Huber et al. in a disease model [19]. This investigation has illustrated how noise can both enhance the responsiveness to weak activations and facilitate the occurrence of aperiodic patterns. On the other hand, from a medical point of view, noise can result in amplification of subclinical vulnerabilities and, thereby, lead to disease onset or transitions to dysrhythmic mood patterns [19].

Much work, addressing specifically the issue of spike time reliability, have shown that it is possible for the spike timing to be reliable through a resonance phenomenon. The results obtained by Fellous et al. on pyramidal cells and interneurons in rat prefrontal cortical slices have demonstrated that subthreshold dynamics of these neurons may act as a band-pass filter [20]. Therefore, maximal reliability was always achieved in the 1:1 entrainment regime. The resonance-related enhancement in spike time reliability was also experimentally observed in Aplysia motoneurons [21,22] and numerically studied for an array of Hodgkin-Huxley-type neurons [23] and for a stochastic θ-neuron [24]. Closely related to the above results, the

[a] e-mail: pankratova_e.v@mail.ru

phenomenon of frequency sensitivity in weak signal detection has been observed in experiments on the cricket cercal sensory system by Levin and Miller [25]. Physically, the existence of such a frequency range is due to the nonlinear resonance between the intrinsic oscillation and the weak periodic signal. When both frequencies match, the input signal can most effectively transfer energy to the neuron to evoke the spiking events [26]. However, this effect was observed for the case of subthreshold forcing, when the driving signal alone is insufficient to produce a response from the neuron, i.e., to generate a spike. In practice, the opposite case of strong driving signals is equally interesting.

In the present paper the influence of both the driving frequency and the noise intensity on the duration of an interspike interval in the output of the classical Hodgkin-Huxley model driven by a suprathreshold forcing is studied. For driving signals in certain frequency ranges (not only the 1:1 range, but also the regime where neuron is 2:1 entrained), we observe how the system can show stable periodic spiking even for relatively large noise intensities. Here, the most accurate transmission of the signal occurs. Outside these frequency ranges, noise of similar intensity destroys the regularity of the spike trains by suppressing the generation of some of the spikes. In this case, the well-known destructive role of noise manifests itself. On the other hand, the periodic order of the neuronal response can be significantly improved by increasing the level of noise within the frequency range where the irregular spiking behavior in the absence of noise is observed. The existence of such a range is known from both numerical [27] and experimental findings [28]. Further we show how noise can regulate the system response for certain frequencies of the periodical driving. We also demonstrate certain peculiarities related to the color of the assumed Gaussian noise source.

2 The model

Let us consider the dynamics of a Hodgkin-Huxley neuronal model described by the following four nonlinear coupled differential equations [29]:

$$\begin{aligned} C_m\dot{V} &= -G_K n^4(V-V_{\rm K}) - G_{\rm Na}m^3h(V-V_{\rm Na}) \\ &\quad - G_L(V-V_L) + I_{ext}(t), \\ \dot{m} &= \alpha_m(1-m) - \beta_m m, \\ \dot{h} &= \alpha_h(1-h) - \beta_h h, \\ \dot{n} &= \alpha_n(1-n) - \beta_n n. \end{aligned} \tag{1}$$

Here C_m is the capacitance of the membrane; $V = V_m - V_{eq}$ is the deviation of the membrane potential V_m from its equilibrium value V_{eq} [30]. The parameters $G_{\rm Na}$, $G_{\rm K}$, and G_L are the maximal conductances for the sodium, potassium and leakage channels, respectively, and $V_{\rm Na}$, $V_{\rm K}$, V_L are the corresponding reversal potentials. The last three kinetic equations in (1) describe the dynamics of the gating variables. Here, m and h are responsible for the activation, respectively the inactivation of the Na^+-current, and n controls the K^+-current activation. The rate functions $\alpha(V)$ and $\beta(V)$ are interpreted as mean transition rates of ionic channels from the closed to the open state, and vice versa. Values of all parameters and functions are given in Appendix A.

In reality neurons always receive inputs from neighboring cells, and there are random fluctuations in the diffusion of neurotransmitters, etc. Any such excitation causes currents to flow through the membrane. This is summed into the total synaptic current. Hence, the total external stimulus received by the neuron is $I_{ext}(t) = A\sin(2\pi ft) + \xi(t)$. Note, that we assume that the sinusoidal component of this input is suprathreshold. This means that, subjected to this periodic drive, the system produces a response even in the noise-free case. In addition, we consider a stochastic component in the input. According to recent experimental results, Gaussian stimulation mimics well the total current to a neuron delivered by the occurrence of many uncorrelated synaptic events [31–33]. The stochastic input to our neuron $\xi(t)$ is therefore modeled as a Gaussian noise and considered as an additive fluctuating current in the first equation of the system (1). In the initial analysis, we consider white Gaussian noise with zero mean $\langle\xi(t)\rangle = 0$ and with the correlation function $\langle\xi(t)\xi(t+\tau)\rangle = D\delta(\tau)$. However, we will also consider colored Gaussian noise.

In the following sections, investigations of the influence of noise on the behavior of system (1) subjected to a signal of amplitude $A = 4\ \mu$ A/cm^2 will be presented. Together with the mean of the interspike duration (ID)

$$T = \langle T\rangle = \lim_{N\to\infty}\frac{1}{N}\sum_{i=1}^{N} T_i \tag{2}$$

we will consider the mean square deviation of ID (SD):

$$SD = \sqrt{\langle T^2\rangle - \langle T\rangle^2}. \tag{3}$$

Here, T_i is the time between subsequent spikes in the system's output. The second moment $\langle T^2\rangle$ is defined in a manner analogous to equation (2). Use of characteristics (2) and (3) allows us to delineate the region, where the most effective noise suppression occurs and, consequently, where the precision of the transferred information is optimal. Additionally, to quantify the variability of the spiking time, we consider a measure that is widely used in the neuroscience literature and which can be deduced from reliable statistics [21,24]. This is the coefficient of variation (CV), that is defined by the following ratio [34,35]:

$$CV = \frac{\sqrt{\langle T^2\rangle - \langle T\rangle^2}}{\langle T\rangle}. \tag{4}$$

This quantity measures the degree of coherence in the system's output and allows to detect the ordering induced by noise within the range of irregular response.

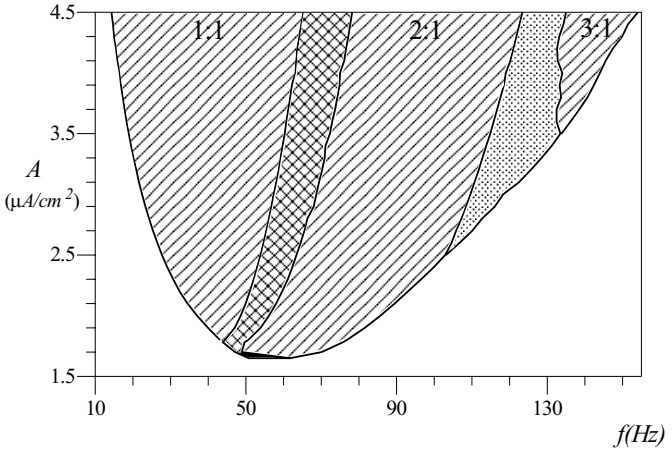

Fig. 1. Parameter space (f, A) illustrating different locking regions of the forced Hodgkin-Huxley neuron for the noise-free case. In the areas marked n:1, one spike occurs for each $n = 1, 2, 3$ periods of the sinusoidal driving. The area between 1:1 and 2:1 contains regions where responses with rational ratios (n:m) occur; in the area between 2:1 and 3:1 the responses are not regular. The white region corresponds to subthreshold forcing signals. For $A = 4$ μA/cm^2 the suprathreshold regime is $f \in (16.5 \div 144$ Hz).

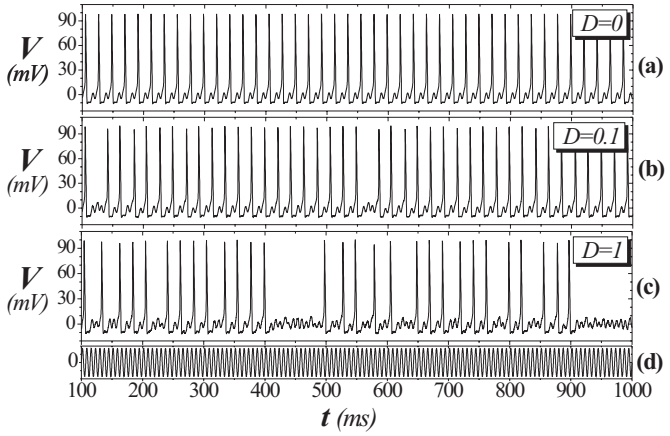

Fig. 2. Voltage profiles induced by an external suprathreshold periodic signal of amplitude $A = 4$ μA/cm^2 for different values of the noise intensity: (a) $D = 0$, (b) $D = 0.1$, and (c) $D = 1$; $f = 140$ Hz. Note, the characteristic phenomenon of spike skipping as the noise intensity increases. The corresponding periodic modulation is shown in (d).

3 Results

3.1 Phase-locking domains

To illustrate the basic locking behavior of the system (1) we start with a brief description of Figure 1, where the regions of various modes of behavior are shown in the frequency vs amplitude parameter space for $D = 0$ (see also [36]). It is known that the mechanism underlying frequency locking is a matching of two time scales: one time scale is the frequency of the external forcing, and the other is that of the damped oscillations around the stable focus of the unforced nerve cell (1). Matsumoto et al. [28] have studied the membrane response of the squid giant axon to an externally applied sinusoidal current. Their results show that different regular and irregular rhythms can be observed, depending on the amplitude and frequency of the applied current. In Figure 1, the different patterns in the system's response are shown with different shading (n:1 pattern means that one spike per n stimulus cycles is observed). The transition from 1:1 to 2:1 occurs through a series of resonances. As it was recently shown by Parmananda et al. [27] for $A = 3$ μA/cm^2, the firing number (ratio of the number of excitations to the number of perturbations) reveals a devil-staircase-like structure. The similar structure, with some peculiarities, is also observed for other amplitudes of suprathreshold periodical driving. As seen from Figure 1, irregular responses occur for amplitudes larger than $A = 2.5$ μA/cm^2, while 3:1 locking is observed for $A > 3.5$ μA/cm^2. Signals with amplitudes smaller than $A \approx 1.6$ μA/cm^2 can not invoke a response for any driving frequency. In this connection it is worth noticing, that the threshold value of the driving amplitude varies with the driving frequency: the threshold value increases both for high and low frequencies. In Figure 1 the subthreshold regime coincides with the non-shaded region.

3.2 The ambiguous role of noise depending on the driving frequency

3.2.1 Destructive role of noise

Let us start by showing a couple of voltage traces. Figure 2 presents the temporal variation of the membrane potential in the absence of noise and when noise of two different intensities, $D = 0.1$ and $D = 1$, is added. Parameters of the periodic driving are: $A = 4$ μA/cm^2 and $f = 140$ Hz. With these parameters our system is subjected to a suprathreshold signal and, in accordance with Figure 1, a periodic chain of spikes is observed. Note, however, that due to the finite response time and the refractive period that follows each spike, only 1/3 of the potential spikes are realized. In the presence of noise a disruption of this periodicity occurs and the skipping of spikes increases with increasing noise intensity. This destructive role of fluctuations in the presence of a suprathreshold signal is well-known and has been demonstrated by several authors both experimentally [25] and in computational models [14–17].

In this section we demonstrate that the negative influence of noise can be effectively suppressed via a proper choice of the driving frequency. With this aim the influence of noise on the process of spike generation is presented in Figure 3 for three different values of the driving frequency $f = 18$ Hz, $f = 60$ Hz, and $f = 140$ Hz with $D = 0.5$. According to Figure 1, all three signals are suprathreshold and, in the deterministic case induce regular periodic spike generation. Moreover, the two signals with the smaller frequencies invoke a system response in the 1:1 regime, while for the highest frequency the system is 3:1 entrained. As

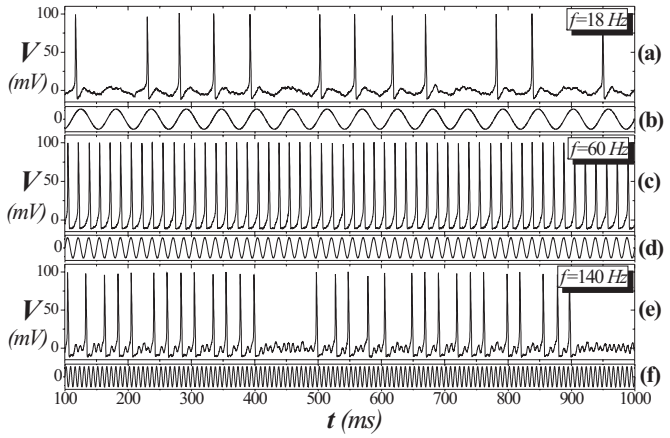

Fig. 3. Voltage profiles induced by an external suprathreshold periodic signal with $A = 4$ μA/cm^2 for different frequencies: (a) $f = 18$ Hz, (c) $f = 60$ Hz, and (e) $f = 140$ Hz. The corresponding periodic modulations are shown in (b), (d), and (f), respectively. $D = 1$. The phenomenon of spike skipping is practically absent for $f = 60$ Hz. For $f = 140$ Hz, on the other hand, only about 23% of the potential spikes are realized.

illustrated in Figure 3, noise suppresses the generation of some spikes but not equally for all frequencies. For instance, around $f = 60$ Hz, the system demonstrates stability to noise: A periodic chain of spikes, as for $D = 0$, is observed, and each period of the forcing signal produces one spike. Here, the transmission of the signal occurs with high reliability.

To get a broader picture, Figure 4 shows computed values of the interspike intervals, normalized to the period of the sinusoidal forcing, as function of the driving frequency for $D = 0$ (a) and $D = 1$ (b), respectively. For the deterministic case, Figure 4a, five different behaviors of the system's response are clearly observed, cf. Figure 1.

By inducing skipping of spikes, noise destroys the regular structure. However, as clearly revealed by Figure 4b, two frequency bands exist where the influence of noise is minimal. In the intervals $f \in (30 \div 60$ Hz) and $f \in (85 \div 105$ Hz), even relatively large values of the noise intensity leave the system's response nearly unaffected. Here, noise leads to a slight shift of the spikes in the voltage traces as reflected in a slight slope of the regions with 1:1 and 2:1 entrainment in Figure 4b. By contrast, the system's response in the region with 3:1 locking demonstrates strong sensitivity to noise. Noise effectively destroys the periodic solution in this region and leads to firing with noticeably larger intervals between the spikes. In this way, fluctuations merge the regions where irregular firing and 3:1 entrainment are observed in the deterministic case. For frequencies outside the region of suprathreshold driving, noise leads to a multimodal distribution of the interval durations. Here, the system's response is sensitive to noise, and fluctuations play an essential role.

Let us now focus on the averaged ID and consider its dependence on the frequency of the external periodic forcing. For the deterministic case the normalized ID, i.e.

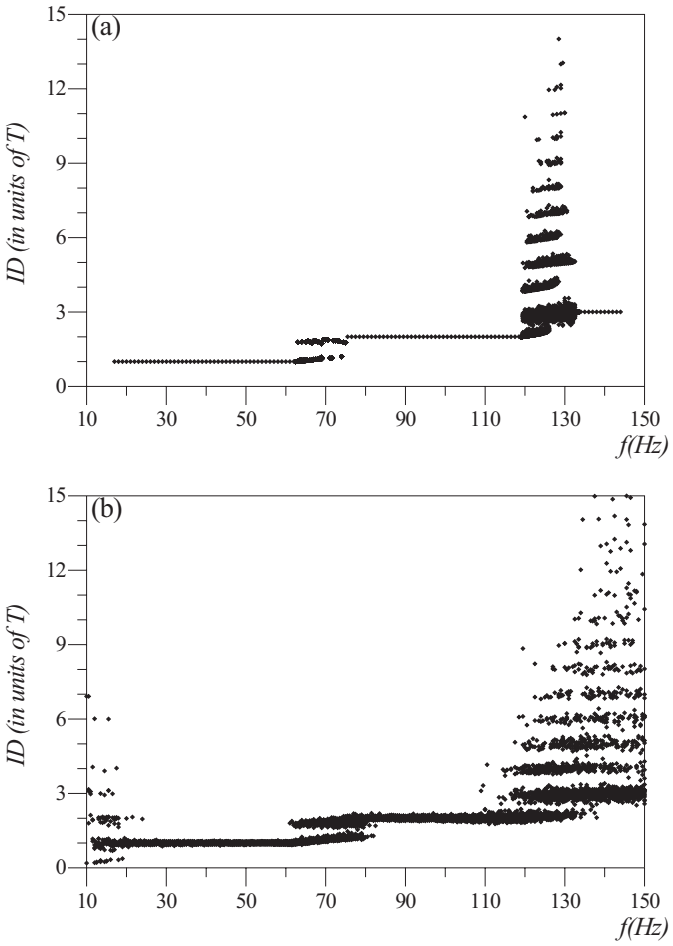

Fig. 4. Bifurcation plot of the normalized interval duration, i.e. T_{ID}/T_s, versus the driving frequency for the deterministic case $D = 0$ (a) and in the presence of noise $D = 1$ (b).

T_{ID}/T_s, has three well-defined horizontal plateaus corresponding to three different phase-locking patterns (solid curve in Fig. 5a). At the same time, the period of the signal T_s decreases as $1/f$ with increasing driving frequency. Consequently, to maintain a constant value, the mean of ID should also decrease with the growth of f. Thus, at the right ends of each plateau, the mean duration of ID should become smaller. For these frequencies of external driving the most rapid generation of spikes in the output of the system occurs.

The mean-square deviation of ID in dependence of the driving frequency is illustrated in Figure 5b. Inspection of this figure shows that the standard deviation of ID (SD) has two deep minima located in the regions of 1:1 and 2:1 patterns, which are much deeper than the minimum corresponding to the 3:1 regime. Moreover, it is seen that, in the small noise limit, the minimum of SD scales as the square root of the noise intensity: $\mathrm{SD}_1/\mathrm{SD}_2 \approx \sqrt{D_1/D_2}$. In a qualitatively similar situation (switching under suprathreshold driving) the similar dependence was observed for the timing errors in the so-called Rapid Single-Flux-Quantum circuits in the presence of thermal noise [37]. Another peculiarity of Figure 5b is a

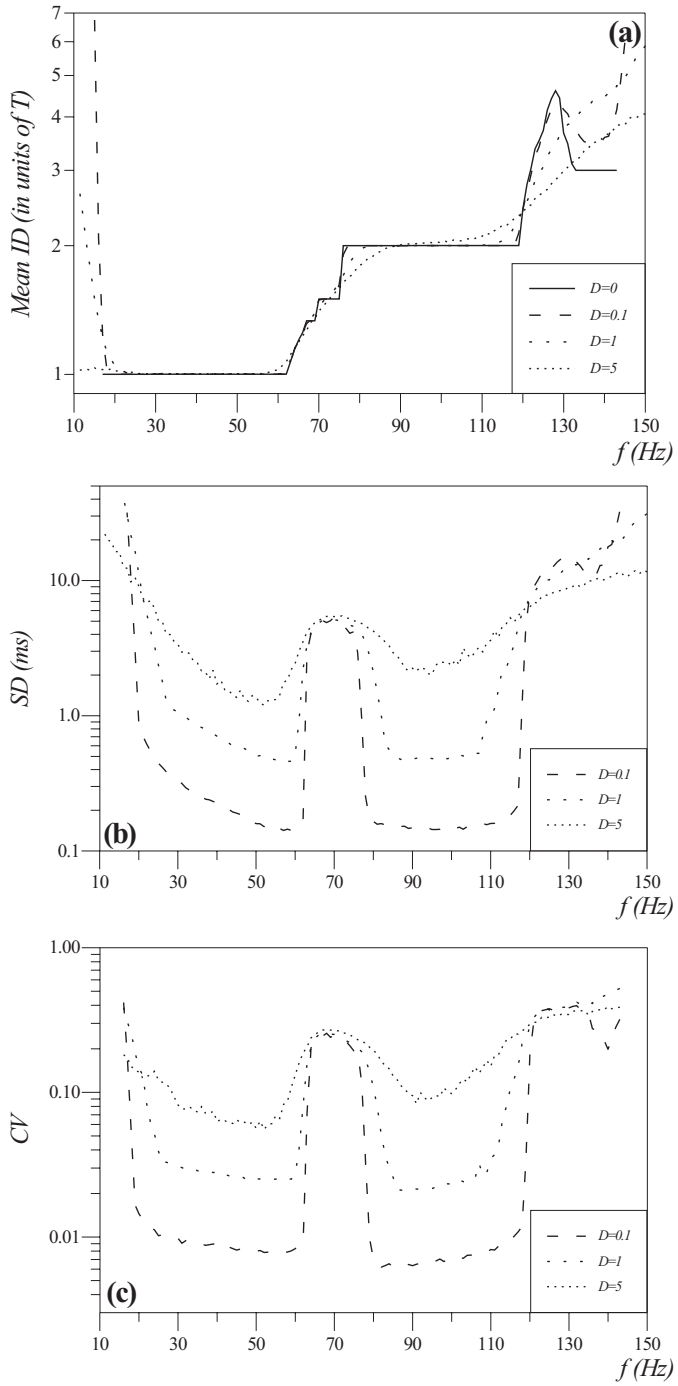

Fig. 5. (a) Mean interval duration, (b) standard deviation, and (c) coefficient of variation as functions of the driving frequency for $A = 4\ \mu\mathrm{A/cm}^2$.

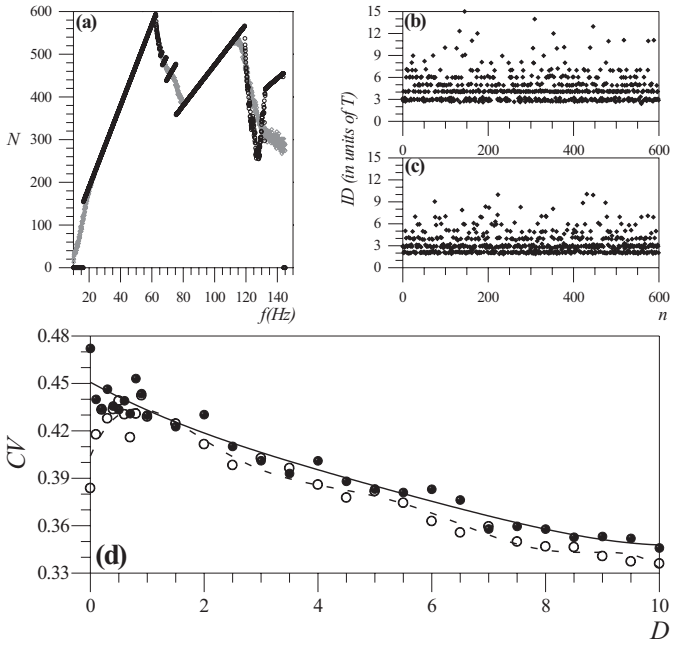

Fig. 6. (a) Number of spikes as a function of the driving frequency for the deterministic case (black circles) and when noise with $D = 1$ is added (gray diamonds). Interval duration versus spike number in the output for (b) $D = 0$ and (c) $D = 1$, $f = 126.5$ Hz. (d) Coefficient of variation (simbols) with interpolations (curves) vs noise intensity for two values of driving frequency: $f = 126.5$ Hz (white circles, dashed line) and $f = 128.5$ Hz (black circles, solid line).

maximum of SD that is observed for the frequency range between regimes with 1:1 and 2:1 locking. This maximum is not produced by the noise alone, but also by the applied calculation method for SD (see Eq. (3)): due to the coexistence of the different IDs within this range (see Fig. 4) this maximum exists even in the noise-free case. It is known that for this range the generation of spike trains is not so reliable as for the 1:1 regime [20,22]. In the following we will not focus on this range, but consider the region where the negative role of noise is minimal. From Figure 5b it is seen, that within the 1:1 range, SD decreases for higher frequencies. Consequently, the effect of noise is significantly reduced in the frequency interval where the most frequent response occurs. This implies that signal transduction will be more effective in this frequency range. The similar dependence for the coefficient of variation in Fig. 5c confirms this fact. In the 2:1 range, SD remains nearly independent of f and increases proportionally with the noise intensity, also indicating the effective suppression of noise.

3.2.2 Constructive role of noise

In this section we consider the frequency range $f \in (119 \div 132$ Hz). As mentioned above (see Fig. 1), this is the range in which irregular responses occur. Even for relatively large noise intensities a similar structure as for $D = 0$ is observed. In the deterministic case, the mean spiking frequency is smaller than the frequency of the driving signal. As seen from Figure 6, fluctuations lead to an increase of the number of spikes in the output of the system and, consequently, to the disappearance of long IDs within this range. As previously described by Huber et al. [19], the presence of noise causes the mean spiking frequency to increase. In our case, for the system driven by a periodic signal, fluctuations cause the mean output frequency to increase and to approach the forcing frequency.

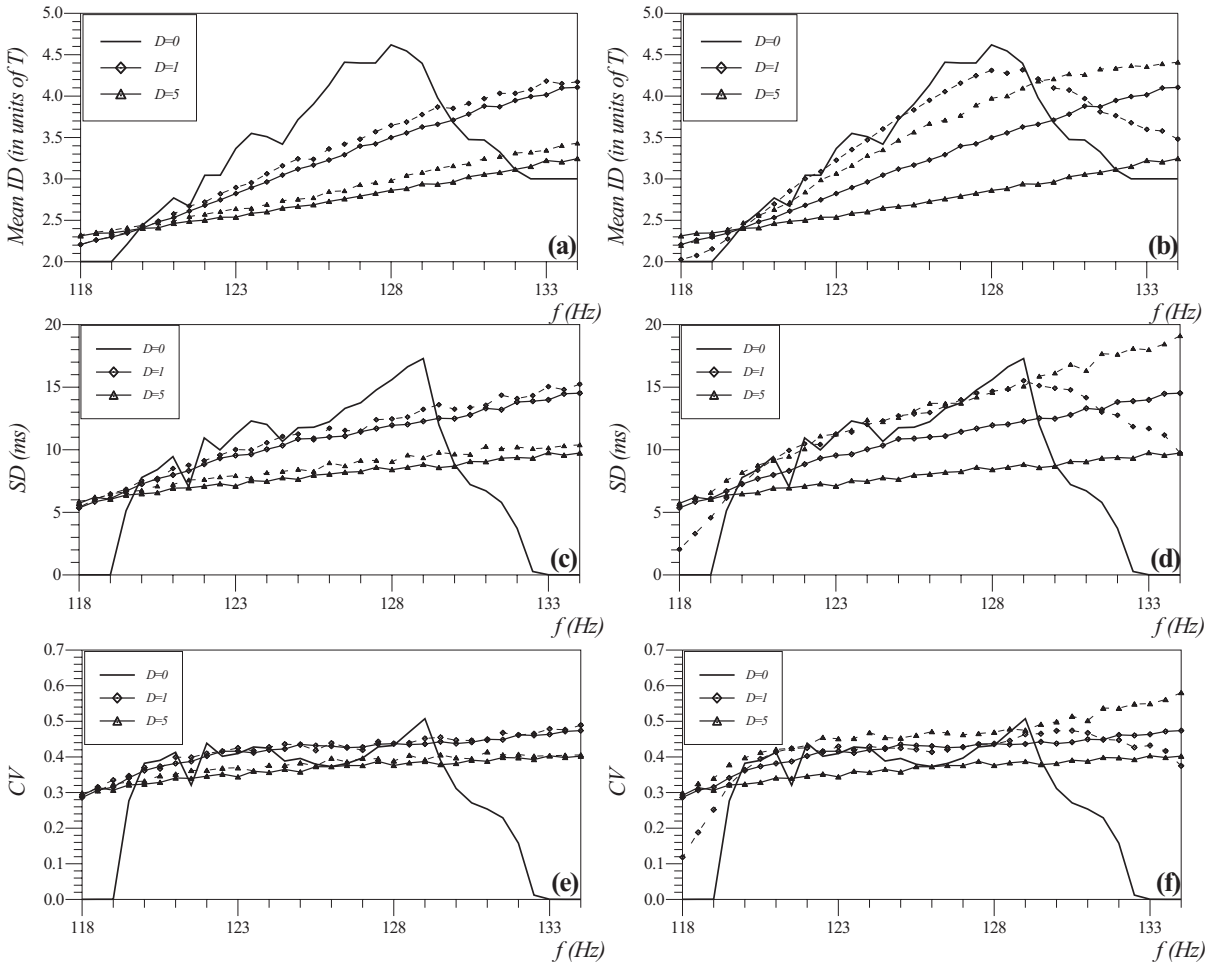

Fig. 7. (a) Mean interspike duration, (c) standard deviation of ID, and (e) coefficient of variation as functions of the driving frequency for $t_c = 1$ ms, $A = 4\ \mu\mathrm{A/cm}^2$. The same dependences for the Ornstein-Uhlenbeck stochastic process with a correlation time $t_c = 10$ ms are shown in (b), (d) and (f). Solid lines correspond to the case of the white Gaussian noise.

From a functional point of view it seems optimal that the two frequencies are as close to one another as possible. We thus conclude that the presence of noise under these circumstances plays a constructive role. To characterize the ordering effect induced by the noise we have calculated the coefficient of variation (CV) for two different frequencies ($f = 126.5$ Hz and $f = 128.5$ Hz) in the range of irregular response. As illustrated in Figure 6d, CV tends to decrease with increasing noise intensity. For some forcing frequencies, this variation is non-monotonic with a maximum at certain noise intensity. However, further increase of the noise always leads to decreasing values of CV. Hence, in this regime, the presence of noise generally enhances the coherence of the neuronal response.

In Figure 7a the mean ID for the deterministic case and for two different values of the intensity of the white Gaussian noise, namely $D = 1$ (diamonds) and $D = 5$ (triangles), is shown by the solid lines. Stronger noise is seen to induce a more ordered behavior of the neuronal response. Note, however, that this phenomenon strongly depends on the driving frequency. Closer inspection of Figure 7a shows a maximal decrease of the mean ID near the frequency $f = 126.5$ Hz. Here, the output frequency significantly increases with the noise amplitude (up to 22.4% for $D = 1$ and 37% for $D = 5$). However, the decrease of SD is not maximal at this frequency. Rather, the minimal variance of the IDs in the output of the system is observed in the vicinity of the driving frequency $f = 128.5$ Hz, Figure 7c. Here, SD changes significantly with increasing noise intensity. Namely, for $D = 1$ SD drops about 32%, and for $D = 5$ the drop is about 50% relative to the deterministic case. For this driving frequency the most precise generation of spikes occurs. The values of coefficient of variation in dependence on driving frequency are shown in Figure 7e.

Let us hereafter examine the role of the color of the noise for the neural response. With this aim we consider system (1) subjected to an Ornstein-Uhlenbeck (OU) stochastic process $\eta(t)$ with zero mean and a correlation function $\langle \eta(t)\eta(t+\tau)\rangle = (D/t_c)\exp(-\tau/t_c)$. This may be

described by the following equation [38]:

$$\frac{d\eta(t)}{dt} = -\frac{\eta(t)}{t_c} + \frac{\xi(t)}{t_c}. \tag{5}$$

Here, as above, $\xi(t)$ is a source of Gaussian white noise with intensity D. The parameter t_c is the correlation time, which is responsible for the bandwidth of the noise (i.e., the color). In the following numerical simulations we consider the same characteristics, namely mean ID, SD and CV (Fig. 7), for two values of the correlation time: $t_c = 1$ ms and $t_c = 10$ ms. In the first case a similar behavior as for the white Gaussian noise is also observed for OU noise (dashed lines in Figs. 7a, 7c, 7e). The percentage relations characterizing the quality of the neuronal response change slightly. In the case $t_c = 10$ ms, however, the bandwidth of the noise becomes narrower. The character of the neural response for driving frequencies where chaotic behavior is observed, is therefore dependent on the high frequency components of the noise spectrum. Increase of the noise intensity here leads to a smaller decrease of the mean ID: about 6% for $D = 1$ and 15% for $D = 5$, Figure 7b. For this type of noise the decrease of SD does not exceed 6% for $D = 1$ and 9.6% for $D = 5$, Figure 7d.

4 Conclusions

The influence of both the driving frequency and the noise intensity on the duration of the interspike interval in the output of a Hodgkin-Huxley model was examined. We observed that for suprathreshold periodic signals with frequencies in the ranges where the neuron is 1:1 or 2:1 entrained, the system can show stable periodic spiking even for relatively large noise intensities. In both of these ranges, the jitter (that is frequently associated with the reliability of transmitted information [20–22]) was low. Thus, the transmission of the signal here occurs with high precision. Outside these frequency ranges, noise of similar intensity destroys the regularity of the spike trains by suppressing the generation of some of the spikes. Here, the well-known destructive role of noise manifests itself.

As it is known from both numerical [27] and experimental studies [28], a frequency range exist where an irregular spiking behavior is observed for periodically stimulated neurons. We have shown that within this range increasing the noise improves the regularity of the system's response. The role of the color of the Gaussian noise source was also examined. The response to noise in the regime of irregular spiking is in principle unpredictable with regard to the duration of interspike intervals. But this time interval displays a clear tendency to a decrease with increasing noise level. This observation allows us to conclude that the constructive role of noise can be of significance from a biological point of view.

This work was partly supported by the European Commission (BioSim, project 005137). E.V.P. and V.N.B. acknowledge support from the Russian Foundation for Basic Research (Projects Nos. 05-01-00509 and 05-02-19815). E.V.P. also acknowledges the support of the Dynasty Foundation.

Appendix A

Parameter values used in the simulations for the Hodgkin-Huxley neuron model are:

C_m	Membrane capacitance	1 μF/cm^2
G_{Na}	Maximal sodium conductance	120 mS/cm^2
G_{K}	Maximal potassium conductance	36 mS/cm^2
G_L	Leakage conductance	0.3 mS/cm^2
V_{Na}	Sodium reversal potential	110 mV
V_{K}	Potassium reversal potential	-12 mV
V_L	Leakage reversal potential	10.6 mV

For these conditions the Hodgkin-Huxley model has a unique globally asymptotically stable equilibrium point which represents the resting state of the cell membrane.

The auxiliary functions $\alpha(V)$ and $\beta(V)$ are given by:

$$\alpha_m = \alpha_{m_0}\frac{V_1 - V}{\exp\left(\frac{V_1 - V}{\vartheta_{m_1}}\right) - 1}, \qquad \beta_m = \beta_{m_0}\exp\left(\frac{-V}{\vartheta_{m_2}}\right), \tag{6}$$

with $\alpha_{m_0} = 0.1(\mathrm{mV\,ms})^{-1}$, $V_1 = 25$ mV, $\vartheta_{m_1} = 10$ mV, $\beta_{m_0} = 4\ (\mathrm{ms})^{-1}$, and $\vartheta_{m_2} = 18$ mV.

$$\alpha_h = \alpha_{h_0}\exp\left(\frac{-V}{\vartheta_{h_1}}\right), \qquad \beta_h = \frac{\beta_{h_0}}{\exp\left(\frac{V_2 - V}{\vartheta_{h_2}}\right) + 1}, \tag{7}$$

with $\alpha_{h_0} = 0.07\ (\mathrm{ms})^{-1}$, $\vartheta_{h_1} = 20$ mV, $\beta_{h_0} = 1\ (\mathrm{ms})^{-1}$, $V_2 = 30$ mV, and $\vartheta_{h_2} = 10$ mV.

$$\alpha_n = \alpha_{n_0}\frac{V_3 - V}{\exp\left(\frac{V_3 - V}{\vartheta_{n_1}}\right) - 1}, \qquad \beta_n = \beta_{n_0}\exp\left(\frac{-V}{\vartheta_{n_2}}\right), \tag{8}$$

with $\alpha_{n_0} = 0.01(\mathrm{mV\,ms})^{-1}$, $V_3 = 10$ mV, $\vartheta_{n_1} = 10$ mV, $\beta_{n_0} = 0.125\ (\mathrm{ms})^{-1}$, and $\vartheta_{n_2} = 80$ mV.

References

1. E.R. Kandel, J.H. Schwartz, T.M. Jessell, *Principles of Neural Science* (Appleton and Lange, Norwalk, 1991)
2. M. Abeles, H. Bergman, E. Margalti, E. Vaadia, J. Neurophysiol. **70**, 1629 (1993)
3. A. Riehle, S. Grün, M. Diesmann, A. Aertsen, Science **278**, 1950 (1997)
4. E.V. Pankratova, A.V. Polovinkin, E. Mosekilde, Eur. Phys. J. B **45**, 391 (2005)
5. H.A. Braun, M.T. Huber, M. Dewald, K. Schäfer, K. Voigt, Int. J. Bifurcation Chaos **8**, 881 (1998)
6. E. Mosekilde, O.V. Sosnovtseva, D. Postnov, H.A. Braun, M.T. Huber, Nonl. Studies **11**, 449 (2004)

7. A. Longtin, Nuovo Cimento D **17**, 835 (1995)
8. A. Longtin, D.R. Chialvo, Phys. Rev. Lett. **81**, 4012 (1997)
9. G.D. Smith, C.L. Cox, S.M. Sherman, J. Rinzel, J. Neurophysiol. **83**, 588 (2000)
10. S. Coombes, M.R. Owen, G.D. Smith, Phys. Rev. E **64**, 041914 (2001)
11. K. Wiesenfeld, F. Moss, Nature **373**, 33 (1995)
12. L. Gammaitoni, P. Hänggi, P. Jung, F. Marchesoni, Rev. Mod. Phys. **70**, 254 (1998)
13. P.E. Greenwood, L.M. Ward, D.F. Russell, A. Neiman, F. Moss, Phys. Rev. Lett. **84**, 4773 (2000)
14. M. DeWeese, W. Bialek, Nuovo Cimento **17D**, 733 (1995)
15. A.R. Bulsara, A. Zador, Phys. Rev. E **54**, R2185 (1996)
16. X. Pei, L. Wilkens, F. Moss, Phys. Rev. Lett. **77**, 4679 (1996)
17. M.T. Huber, H.A. Braun, Proceedings of SPIE **5110**, 332 (2003)
18. N.G. Stocks, in *Stochastic Processes in Physics, Chemistry and Biology*, edited by J.A. Freund, T. Poschel, Lecture Notes in Physics, LNP 557 (Springer-Verlag, Berlin, 2000), pp. 150–159
19. M.T. Huber, H.A. Braun, J.C. Krieg, Biol. Psychiatry **47**, 634 (2000)
20. J.-M. Fellous, A.R. Houweling, R.H. Modi, R.P.N. Rao, P.H.E. Tiesinga, T.J. Sejnowski, J. Neurophysiol. **85**, 1782 (2001)
21. J.D. Hunter, J.G. Milton, P.J. Thomas, J.D. Cowan, J. Neurophysiol. **80**, 1427 (1998)
22. J.D. Hunter, J.G. Milton, J. Neurophysiol. **90**, 387 (2003)
23. Y. Yu, F. Liu, J. Wang, W. Wang, Phys. Lett. A **282**, 23 (2001)
24. B. Gutkin, G.B. Ermentrout, M. Rudolph, J. Comp. Neuroscience **15**, 91 (2003)
25. J.E. Levin, J.P. Miller, Nature **380**, 165 (1996)
26. W. Wang, Y. Wang, Z.D. Wang, Phys. Rev. E **57**, R2527 (1998)
27. P. Parmananda, C.H. Mena, G. Baier, Phys. Rev. E **66**, 047202 (2002)
28. G. Matsumoto, K. Aihara, Y. Hanyu, N. Takahashi, S. Yoshizawa, J. Nagumo, Phys. Lett. A **123**, 162 (1987)
29. A.L. Hodgkin, A.F. Huxley, J. Physiology **117**, 500 (1952)
30. J. Keener, J. Sneyd, *Mathematical Physiology* (Springer Verlag, Berlin, 1998)
31. Z.F. Mainen, T.J. Sejnowski, Science **268**, 1503 (1995)
32. M. Juusola, A.S. French, Neuron **18**, 959 (1997)
33. F. Liu, W. Wang, X. Yao, Biol. Cybern. **77**, 217 (1997)
34. A.S. Pikovsky, J. Kurths, Phys. Rev. Lett. **78**, 775 (1997)
35. B. Lindner, J. Garcia-Ojalvo, A. Neiman, L. Schimansky-Geier, Phys. Rep. **392**, 321 (2004)
36. S.-G. Lee, S. Kim, Phys. Rev. E **60**, 826 (1999)
37. A.V. Rylyakov, K.K. Likharev, IEEE Trans. Appl. Supercond. **9**, 3539 (1999)
38. C.W. Gardiner, *Handbook of Stochastic Methods*, 2nd edn. (Springer, Berlin, 1985)